

Materials and characterization methods

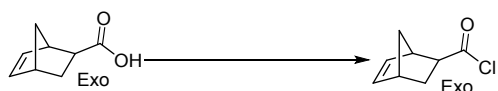
All reactions were performed in an argon-filled glovebox ($O_2 < 2$ ppm, $H_2O < 0.5$ ppm) at room temperature using oven-dried glassware. THF, toluene, and DCM was dried using a commercial solvent purification system. rac-Lactide {Aldrich}, sec-butyllithium solution {1.3 mol/L in cyclohexane/hexane (92/8), ACROS Organics} and ethylene oxide solution (2.5-3.3 mol/L in THF, Aldrich) was used as received. 1,8-diazabicyclo[5.4.0]undec-7-ene (DBU) {Aldrich} was distilled over CaH_2 and storage under argon at -20 °C. Styrene was pass through neutral alumina plug and stored under argon at -20 °C. $[(H_2IMes)(3-Brpy)_2(Cl)_2Ru=CHPh]$, G3 was synthesized according to literature.¹ exo-5-Norbornene-2-carboxylic acid and exo-5-Norbornene-2-methanol was synthesized according to literature.²

Nuclear Magnetic Resonance (NMR) spectra were recorded on a Bruker AVANCE III 500 MHz spectrometer. Spectra are reported in ppm and referenced to the residual solvent signal: $CDCl_3$ (1H 7.26 ppm, ^{13}C 77.16 ppm).

Conventional Gel Permeation Chromatography (GPC) was performed using a Tosoh Ecosec HLC-8320GPC at 40 °C fitted with a guard column (6.0 mm ID x 4.0 cm), and two analytical columns (TSKgel GMH_{HR}-H, 7.8 mm ID x 30 cm x 5 μ m). A flow rate of 1.0 mL·min⁻¹ was used. THF (HPLC grade) was used as the eluent, and polystyrene standards (15 points ranging from 500 Mw to 8.42 million Mw) were used as the general calibration. An additional calibration was created for specifically for linear polylactic acid and only used for linear polylactic acid (10 points ranging from 500 Mw to 10,000 Mw). UV detector was recorded at 266 nm.

Absolute molecular weight was obtained with a Tosoh Ecosec HLC-8320GPC and LenS3 Multi-Angle Light Scattering Detector at 40 °C fitted with a guard column (6.0 mm ID x 4.0 cm x 5 μ m), and two analytical columns (TSKgel Alpha-M, 7.8 mm ID x 30 cm). THF (HPLC grade) was used as the eluent and a flow rate of 0.6 mL·min⁻¹ was used. The detectors were calibrated with a narrow polystyrene standard (Mw= 99,000 Da). Polymer solutions were prepared at a known concentration (ca. 3 mg/mL) and an injection volume of 20 μ L was used. dn/dc values for the bottlebrush polymers were obtained for each injection by assuming 100% mass elution from the columns.

Procedure for the synthesis of exo-5-norbornene-2-acid chloride



In a round bottom flask attached to an argon line, exo-5-Norbornene-2-carboxylic acid (5.00 g, 36.2 mmol) was dissolved into 100 ml of dry DCM. The reaction was cooled to 0 °C with an ice bath and a small amount of DMF (5 drops, ~ 0.1 ml) was added to the reaction mixture. In a separate flask under argon, oxalyl chloride (5.06 g, 3.4 ml, 39.9 mmol) was dissolved into DCM (20 ml). The oxalyl chloride solution was added dropwise to the carboxylic acid flask over 20 mins. Upon completion of the addition, the ice bath was removed and the reaction was allowed to stir overnight at room temperature. The reaction was then placed under vacuum (~1 torr) to concentrate the solution. After the solvent was removed, vacuum distillation was performed to collect the product (4.4 g, yield: 78%) as a colorless liquid. 1H NMR (500 MHz, $CDCl_3$): δ = 6.21(dd, J =3.0, 5.7 Hz, 1H), 6.13 (dd, J =3.1, 5.7 Hz, 1H), 3.29 (s, 1H), 2.99 (s, 1H), 2.74 (ddd, J =1.6, 4.7, 9.0, 1H), 2.02 (ddd, J =3.6, 4.7, 12.0, 1H), 1.5 (m, 3H). ^{13}C { 1H } NMR (125 MHz, $CDCl_3$): δ = 177, 139, 135, 57, 47, 46, 42, 31.

1H NMR data is consistent with prior literature.³

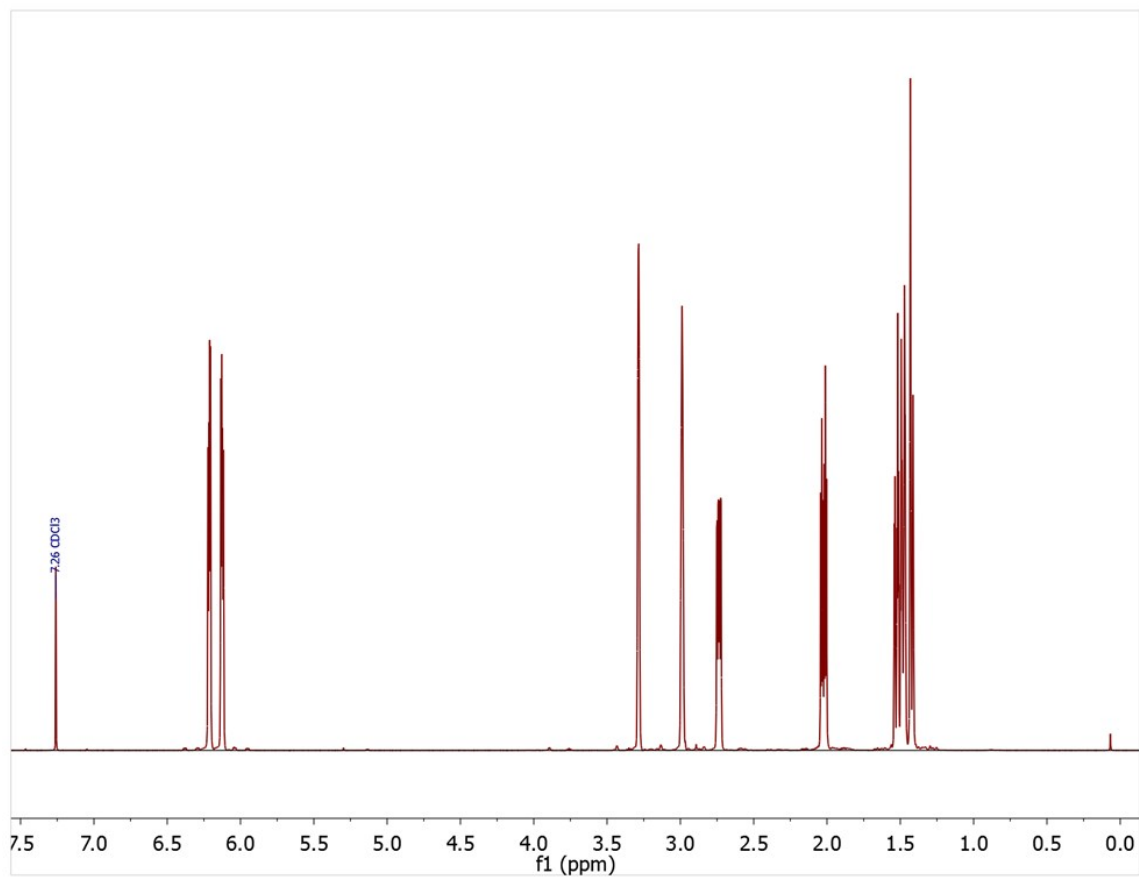


Figure S1: ^1H NMR of exo-5-norbornene-2-acid chloride in CDCl_3 .

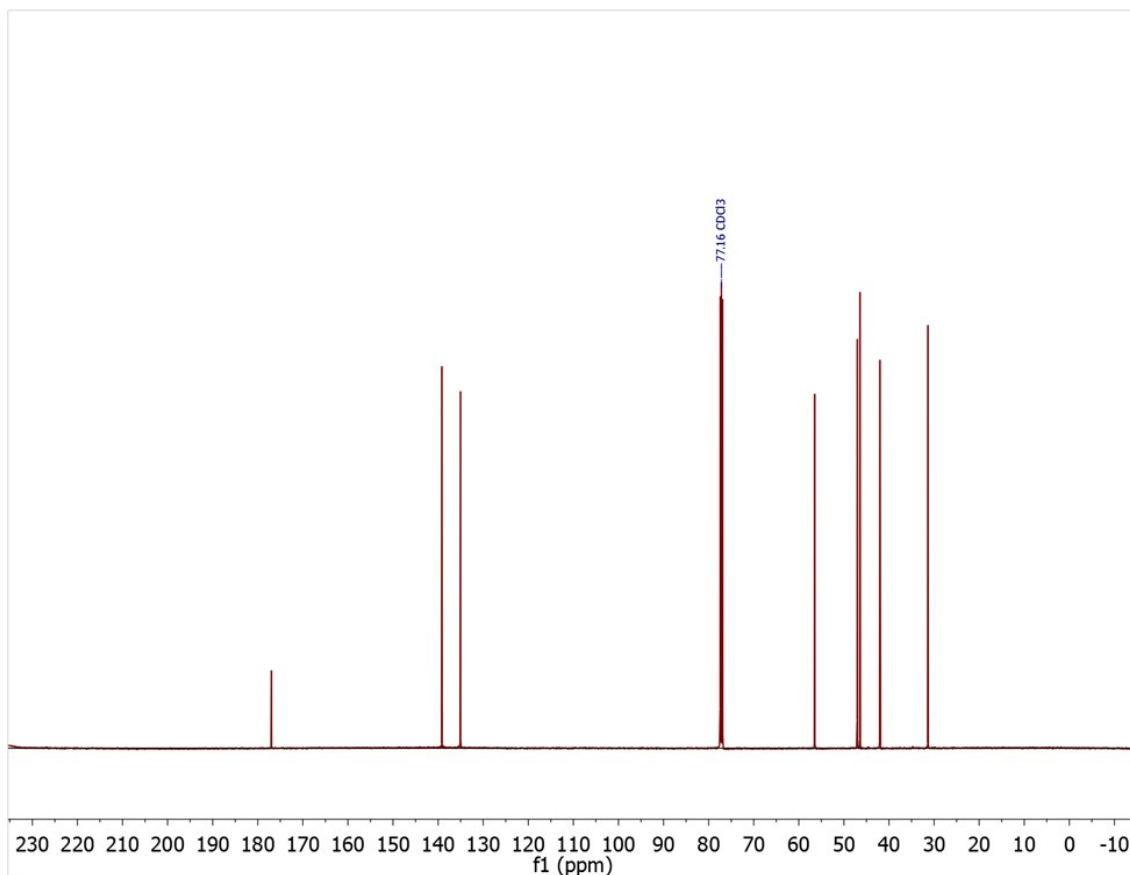
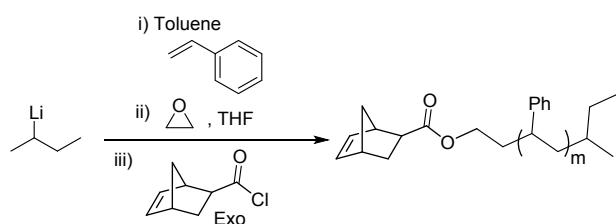


Figure S2: ^{13}C NMR of exo-5-norbornene-2-acid chloride in CDCl_3 .

Synthesis of PS macromonomers



Procedure for the synthesis of PS macromonomers

In an argon filled glovebox, a round bottom flask was filled with 220 ml of dried toluene. The solution of secBuLi (3 ml, 3.9 mmol) was added next, followed by styrene (18.3 g, 176 mmol) to initiate the polymerization. The reaction mixture immediately turned orange. After 30 min, ethylene oxide solution (1.95 ml, 5.85 mmol) was added, which immediately resulted in the solution going colorless. After 30 min, exo-5-norbornene-2-acid chloride (794 mg, 5.07 mmol) was added. The reaction was allowed to stir overnight, in which a small amount of white solid formed. The polymer was isolated by precipitation in methanol 3 times and dried under vacuum. $M_n(\text{GPC}) = 4,500 \text{ g/mol}$; $\bar{D} = 1.03$

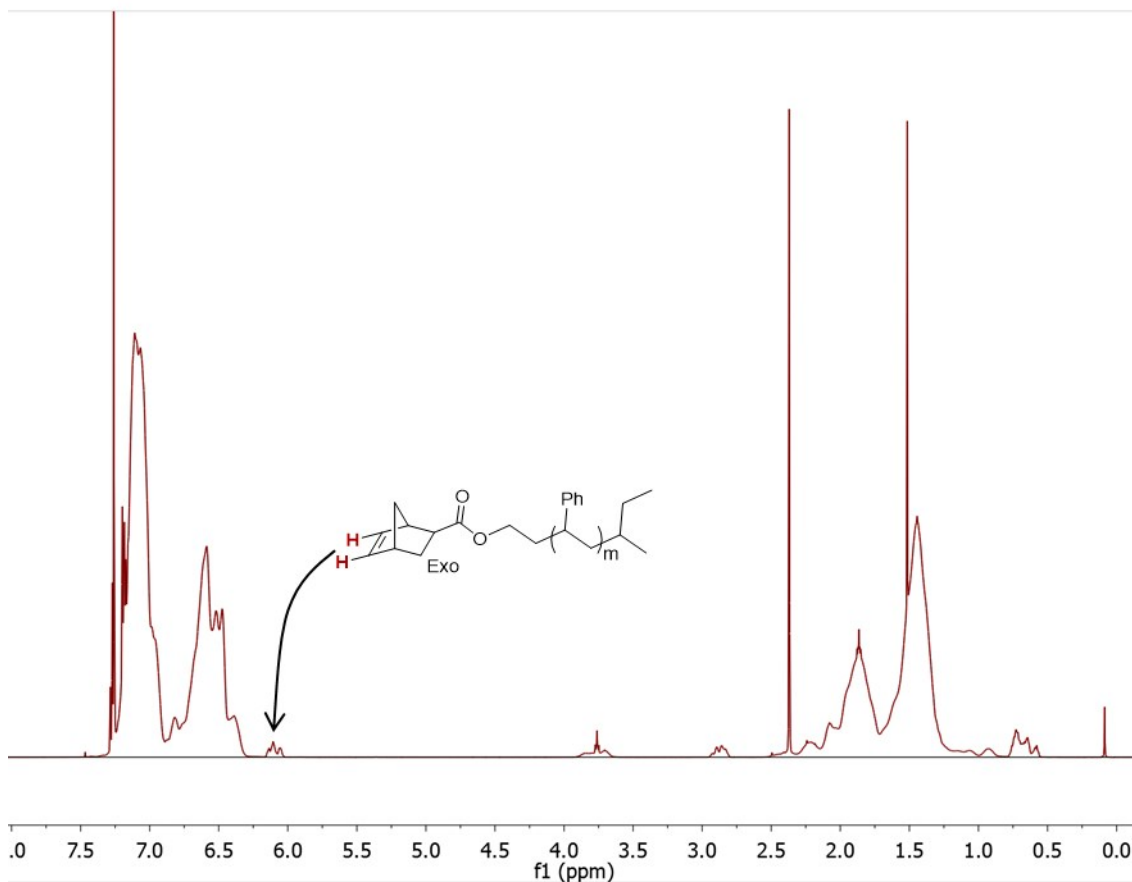
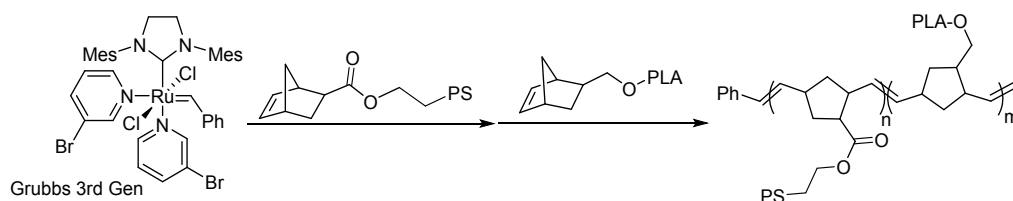


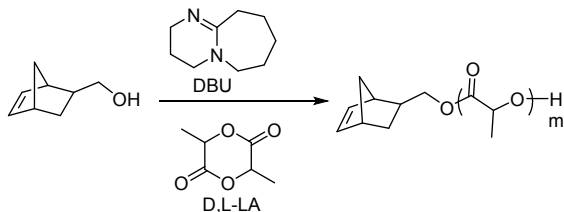
Figure S3: ^1H NMR of PS macromonomer (4.5 kg/mol) in CDCl_3 .

Representative synthesis of PS-b-PLA bottlebrush polymers



The synthesis of PLA macromonomers was performed just prior to the diblock bottlebrush synthesis so that the quenched ROP reaction mixture could be added directly into the graft-through ROMP polymerizations to form the second block. This method was used instead of isolated PLA macromonomers because low molecular weights ($< 5,000$ g/mol) do not precipitate well, making it challenging to recover pure PLA macromonomers.

→ **Procedure for the synthesis of PLA macromonomers**



The procedure for the ring opening polymerization (ROP) of lactide has been adapted from the previous work of our group.^{4,5}

To an oven-dried 20 mL glass vial, lactide (1.4g, 9.71 mmol) and exo-5-Norbornene-2-methanol (30.2 mg, 0.243 mmol) dissolved in 8.7 mL of THF. The polymerization was initiated by adding DBU (7.38 mg, 0.0485 mmol) dissolved in 1 mL of THF. This reaction mix for 60 min at which time $B(OH)_3$ (60.0 mg, 0.969 mmol) in 4 ml of THF was added to the reaction mixture. An aliquot was removed for GPC and NMR analysis. (This crude reaction mixture will contain 1g of PLA macromonomers and will be added directly into the graft-through ROMP.) $M_n(\text{GPC}) = 4,200$ g/mol; $D = 1.05$.

Note: In order to get $B(OH)_3$ to dissolve into THF, the solution was heated to $\sim 80-90$ °C till all the $B(OH)_3$ dissolved and allowed to cool back to room temperature before use. Avoid rapid cooling of the solution, as it will cause $B(OH)_3$ to drop out of solution

→ Procedure for the graft-through ROMP

In an oven-dried 20 mL glass vial, PS macromonomer (1000 mg, 0.22) was dissolved into THF (6 ml). The polymerization is initiated by adding G3 via a stock solution (0.5 ml add of: 5 mg G3 in 2.55 ml THF stock solution; 0.98 mg, 0.0011 mmol resulting in a total backbone length 400). After 10 mins, an aliquot was taken and injected into 1 ml of THF with a large excess of ethyl vinyl ether for GPC analysis of the first block. Then, the crude PLA macromonomer from above was added and allow to react for 30 min before a large excess of vinyl ether was added. The polymer was obtained by precipitating into methanol twice and dried under vacuum.

Table S1: Characterization data for PS-PLA diblock bottlebrush (PS: 4.5 kg/mol; PLA: 4.2 kg/mol, 50 wt% PS).

N_{bb}	M_n^a (kg/mol)	M_w/M_n^a	Macromonomer Conv. ^b	wt % ^c				Block length PS:PLA	$M_{n, \text{GPC}}^d$ (kg/mol)	M_w/M_n^d
				Diblock BB	Block 1	PLA Brush	PS Brush			
400	610	1.03	>98%	94	4	>1	2	196:210	1690	1.06

^aCalculated with respect to PS standards ^bDetermined from ¹H NMR; disappearance of norbornene alkene signals ~ 6.2 ppm (includes both PS and PLA). ^cSee SI section ##. ^dDetermined from light scattering GPC

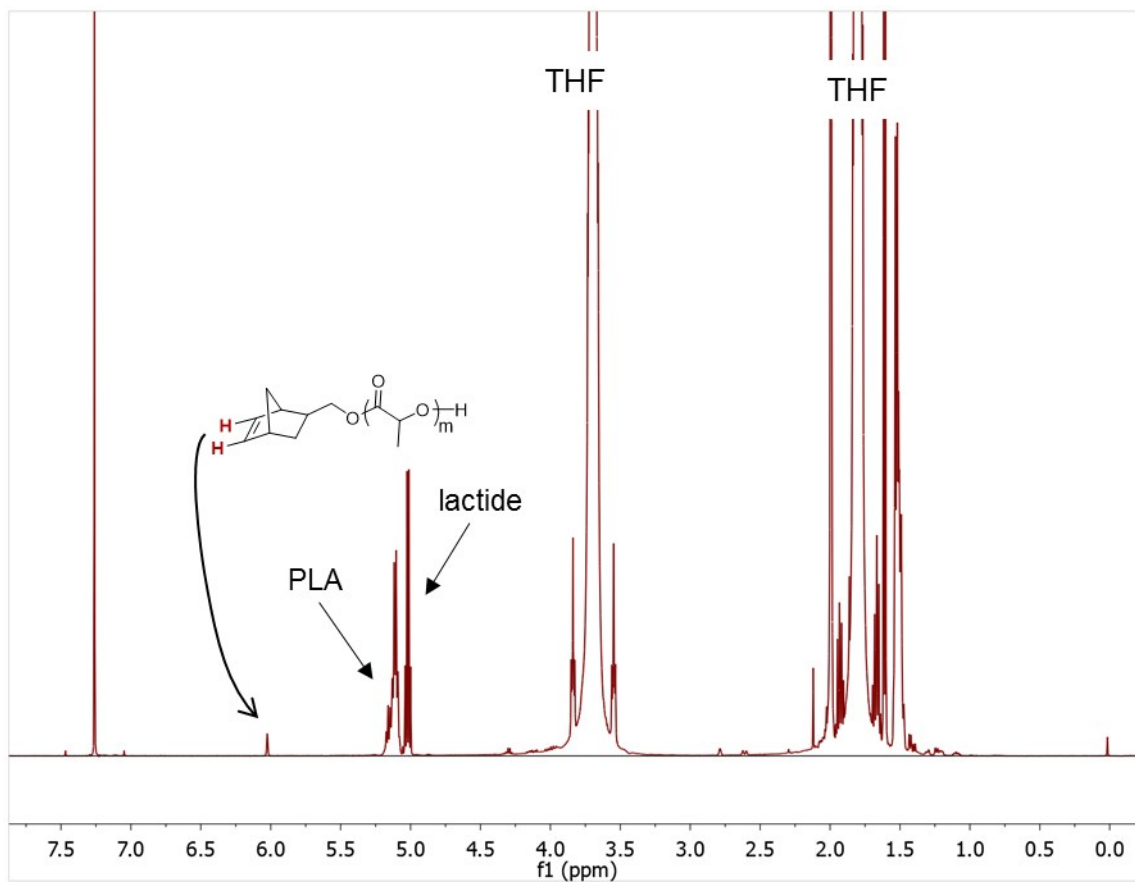


Figure S4: ¹H NMR of an aliquot from crude reaction mixture for the synthesis of PLA macromonomer (4.2 kg/mol) CDCl₃.

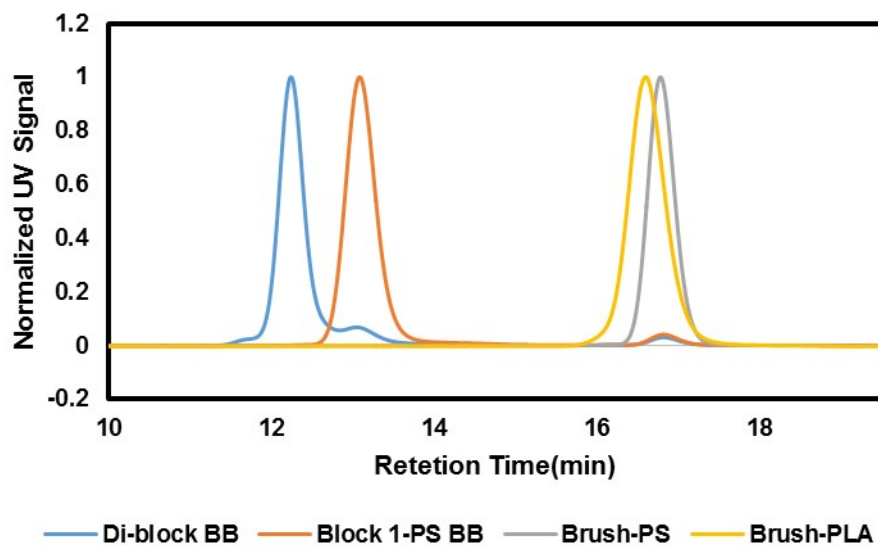


Figure S5: UV-GPC traces for the synthesis of PS-b-PLA diblock bottlebrush.

Procedure for to calculate impurities in diblock bottlebrush sample

From the RI-GPC (**Figure S5**) it is apparent that there are two contaminants of the PS-*b*-PLA bottlebrush. The first impurity is linear polystyrene which does not contain a norbornene end-group. This was deduced from the fact that the impurity is observed at the end of the ROMP of the first block which was only PS (and is the same height in diblock), and from the fact that the NMR shows no alkene signals (detection limit was determined to be >98% conversion).⁴ The second impurity is PS-BB, which is suspected to form from impurities introduced with the addition of PLA macromonomers, which terminated to growing BB chain.

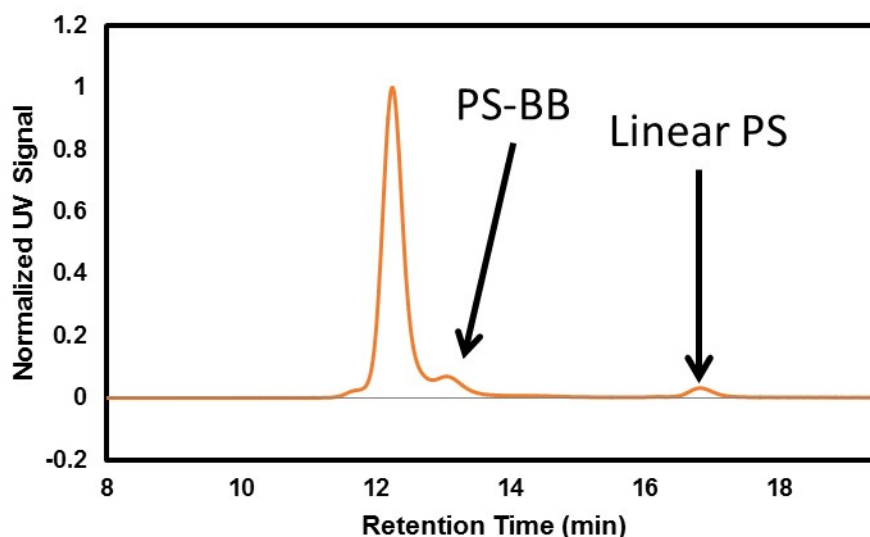


Figure S6: Labeled UV-GPC traces of PS-*b*-PLA bottlebrush.

To quantify the level of impurity of the final PS-*b*-PLLA bottlebrush sample we elected to analyze the UV-GPC trace of the sample. The UV wavelength was chosen to be 266 nm as PLA has no absorbance in this range and PS has a high absorbance (Table S6). Thus our UV-GPC only shows PS. Determining the area under each of the 3 peaks will provide a PS ratio between all the polymers which can be used to determine weight percent contamination levels.

Table S2: Data for PLA and PS response on RI and UV GPC detectors (7.5 mg/ml THF).

UV (nm)	PLA		PS	
	Area RI	Area UV	Area RI	Area UV
200	1393	390	5528	2920
233	1402	1020	5551	2019
266	1411	<10	5542	4580
300	1410	<10	5539	11
325	1411	<10	5593	<10
350	1420	<10	5541	<10

To accurately determine the area under the curve, 3 Gaussian distributions were fitted to the UV-GPC trace. **Figure S7** shows the original trace and the 3 individual Gaussian fits.

$$\text{gaussian distribution } f(x) = \frac{\alpha}{\sigma\sqrt{2\pi}} \exp\left(-\frac{(x-\mu)^2}{2\sigma^2}\right)$$

α = height fitting parameter

σ = standard deviation

μ = center position of distribution (average value)

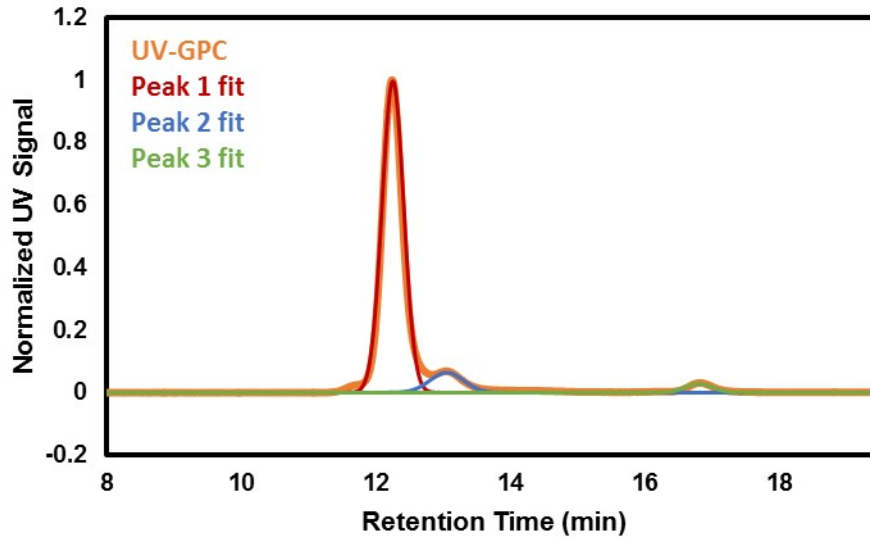


Figure S7: Fitted Gaussian distribution and UV-GPC trace for PS-b-PLA bottlebrush.

The area of the Gaussian distributions was calculated with the equation below.

$$\text{Area} = \int_a^b \frac{\alpha}{\sigma\sqrt{2\pi}} \exp\left(-\frac{(x-\mu)^2}{2\sigma^2}\right) dx = \left(\frac{\alpha}{\sigma\sqrt{2\pi}}\right) \left(\frac{\sqrt{\pi}}{2\sigma}\right) \left(\text{erf}\left(\frac{\mu-a}{\sqrt{2}\sigma}\right) - \text{erf}\left(\frac{\mu-b}{\sqrt{2}\sigma}\right)\right)$$

With the area calculated, the mole percent was calculated followed by weight percent. The final results are shown in **Table S3**.

$$\text{mol\% diblock } BB = M\%_{BB} = \frac{(A_{BB} * N_{block})}{(A_{BB} * N_{block}) + (A_{block1} * N_{block}) + (A_{brush})}$$

$$\text{mol\% block1} = M\%_{block1} = \frac{(A_{block1} * N_{block})}{(A_{BB} * N_{block}) + (A_{block1} * N_{block}) + (A_{brush})}$$

$$\text{mol\% brush} = M\%_{brush} = \frac{(A_{brush})}{(A_{BB} * N_{block}) + (A_{block1} * N_{block}) + (A_{brush})}$$

A_{BB} = UV - GPC Area for di - block bottlebrush

A_{block1} = UV - GPC Area for block1

A_{brush} = UV - GPC Area for brush

N_{block} = Degree of polymerization of block1 (200 units for the example)

$$wt \% \text{ diblock BB} = \frac{(M\%_{BB} * MW_{BB})}{(M\%_{BB} * MW_{BB}) + (M\%_{block1} * MW_{block1}) + (M\%_{brush} * MW_{brush})}$$

$$wt \% \text{ block1} = \frac{(M\%_{block1} * MW_{block1})}{(M\%_{BB} * MW_{BB}) + (M\%_{block1} * MW_{block1}) + (M\%_{brush} * MW_{brush})}$$

$$wt \% \text{ brush} = \frac{(M\%_{brush} * MW_{brush})}{(M\%_{BB} * MW_{BB}) + (M\%_{block1} * MW_{block1}) + (M\%_{brush} * MW_{brush})}$$

MW_{BB} = Molecular weight of di - block bottlebrush = $MW_{brush1} * N_{block1} + MW_{brush2} * N_{block2}$

MW_{block1} = Molecular weight of block1 = $MW_{brush1} * N_{block1}$

MW_{brush} = Molecular weight of brush (from GPC)

Table S3: Data for UV-GPC trace Gaussian distribution fitting, area, and weight %.

	di-block BB	first block	brush
μ	12.25	13.05	16.8
σ	0.16	0.25	0.2
α	0.4	0.04	0.014

Considering the Impact of Deuterated Solvents

Lopez-Barron, et al demonstrated the differences between protonated and deuterated solvents can have a significant impact on the assembly of worm-like micelles⁶. We characterized the linear rheology and steady shear response of PS-PLA diblock bottlebrush dispersed in both solvents to confirm that the differences between protonated and deuterated toluene did not have any significant impact on the reported observations. Measurements for the protonated toluene sample were carried out on an Anton-Paar MCR 702 with a 43 mm parallel plate, while measurements for the deuterated toluene sample were conducted on an Anton-Paar MCR 501 in a Couette cell with a 50 mm cup and a 48 mm bob. As can be seen in figure S8, both the frequency and flow sweeps were found to be comparable with similar trends across the tested range of shear rates and frequencies. Data are observed to be offset by approximately 30%, which is comparable to observations made by Lopez-Barron, et al and Mukerjee, et al^{6,7}.

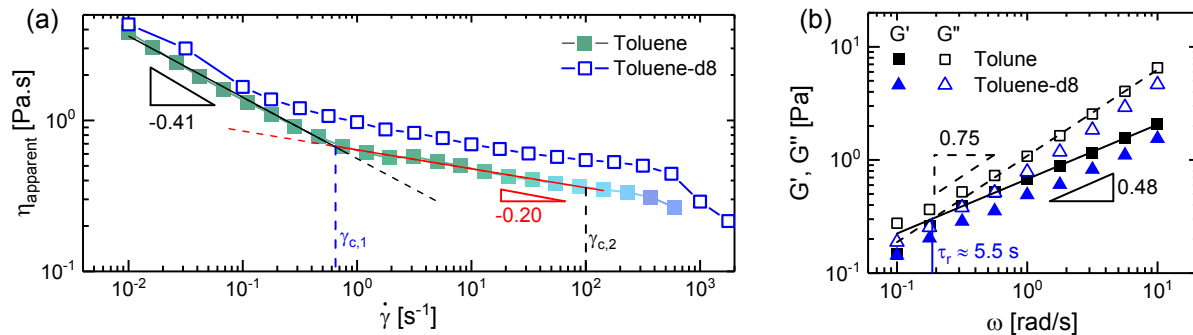


Figure S8: (a) Flow sweeps for polymer dispersed in toluene and toluene-d8. (b) Frequency sweeps for polymer dispersed in toluene and toluene-d8.

Analyzing 2D Small Angle Neutron Scattering Data

Azimuthal and sector averages were performed to quantify the exact location, width, and azimuthal smearing of the peaks observed in the 2D scattering data. Diagrams depicting how these averages were performed are shown in figure S9. Azimuthal averages were centered at the peaks located at q^* and q_p to quantify the alignment of the bottlebrushes and the alignment of the self-assembled lamellae, respectively. The width of the average was set to 0.01 \AA^{-1} when centered at q^* and 0.001 \AA^{-1} when centered at q_p such that the majority of the peak was captured when performing the average. Sector averages were carried out across the entire q range, encompassing data located on both the front and back set of detectors. The width of the sector averages was set to 15° to the center of the peak while simultaneously limiting the effects of azimuthal smearing on the average. Sector averages were conducted along the gradient direction in the 2-3 scattering plane and along the vorticity direction in the 1-3 scattering plane. Sector averages were also taken along the vorticity direction in the 2-3 scattering plane but were found to match the sector averages taken in the 1-3 plane. As such these sector averages are not reported. All averages and data reduction were conducted SANS reduction software protocols provided by NIST⁸.

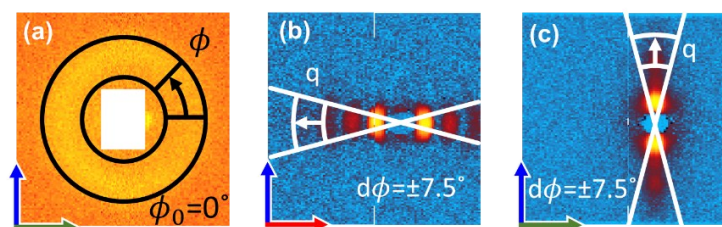


Figure S9: Blown up inset images from figures 8, 10 a, and 10 b highlighting the region on the 2D scattering data characterized by (a) azimuthal sweeps, (b) sector averages at 0° , and (c) sector averages at 90° .

To quantify how shear rate affected the exact location of the primary lamellae peak and relative dispersity of the lamellae spacing, 5 gaussian peaks were fit to the sector averages taken along the gradient and vorticity directions as shown in figure S10. A constant baseline was used during this fitting to simplify the fitting process. The value of this baseline was selected such that the 5th peak, q^* , corresponding to the interaction distance between bottlebrush backbones was isolated from the other peaks. Characterization of the lamellae spacing and dispersity was done carried out with the primary lamellae peak q_p due to the calculated standard error reported by OriginPro being significantly higher for the higher order peaks.

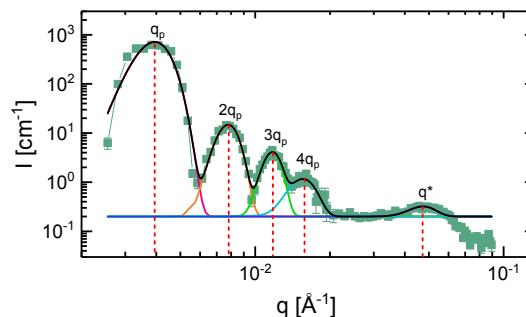


Figure S10. 5 gaussian peaks fit to the sector average taken during quiescence in the 2-3 originally plotted in figure 9 (a). The term q_p represents the primary lamellar peak with subsequent peaks labeled according to the integer multiple. The peak labeled q^* corresponds to the intramolecular interaction peak observed at high q . Red dashed lines serve as guides to the eye, highlighting the location of the peak center.

Disclaimer

Any mention of commercial products in this manuscript are for information only and does not imply endorsement by NIST.

References

- 1 J. A. Love, J. P. Morgan, T. M. Trnka and R. H. Grubbs, *Angew. Chemie Int. Ed.*, 2002, **41**, 4035–4037.
- 2 S. C. Radzinski, J. C. Foster, R. C. Chapleski, D. Troya and J. B. Matson, *J. Am. Chem. Soc.*, 2016, **138**, 6998–7004.
- 3 C. Pugh, J. Y. Bae, J. Dharia, J. J. Ge and S. Z. D. Cheng, *Macromolecules*, 1998, **31**, 5188–5200.
- 4 D. J. Walsh and D. Guironnet, *Proc. Natl. Acad. Sci.*, 2019, **116**, 1538–1542.
- 5 S. Dutta, M. A. Wade, D. J. Walsh, D. Guironnet, S. A. Rogers and C. E. Sing, *Soft Matter*, 2019, **15**, 2928–2941.
- 6 C. R. López-Barrón and N. J. Wagner, *Soft Matter*, 2011, **7**, 10856.
- 7 P. Mukerjee, P. Kapauan and H. G. Meyer, *J. Phys. Chem.*, 1966, **70**, 783–786.
- 8 S. R. Kline, *J. Appl. Crystallogr.*, 2006, **39**, 895–900.